



Comparison of Overcharge Behavior of AlPO_4 -Coated LiCoO_2 and $\text{LiNi}_{0.8}\text{Co}_{0.1}\text{Mn}_{0.1}\text{O}_2$ Cathode Materials in Li-Ion Cells

Jaephil Cho,^{a,*} Hyemin Kim,^b and Byungwoo Park^{b,*}

^aDepartment of Applied Chemistry, Kumoh National Institute of Technology, Gumi, Korea

^bSchool of Materials Science and Engineering, and Research Center for Energy Conversion and Storage, Seoul National University, Seoul, Korea

The overcharge behavior of AlPO_4 -coated $\text{Li}_x\text{Ni}_{0.8}\text{Co}_{0.1}\text{Mn}_{0.1}\text{O}_2$ cathodes was compared to that of AlPO_4 -coated Li_xCoO_2 cathodes in Li-ion cells. The former exhibited less heat generation than the latter as the charge voltage increased. Moreover, the coated $\text{Li}_x\text{Ni}_{0.8}\text{Co}_{0.1}\text{Mn}_{0.1}\text{O}_2$ cathode showed two distinct sets of exothermic peaks beginning at ~ 75 and $\sim 200^\circ\text{C}$, respectively, while the coated Li_xCoO_2 exhibited relatively continuously increasing exothermic peak beginning at $\sim 150^\circ\text{C}$. The results were consistent with the 12 V overcharge tests using Li-ion full cells. As the C rate increased from 1 to 3 C, the cell-surface temperature with the AlPO_4 -coated $\text{Li}_x\text{Ni}_{0.8}\text{Co}_{0.1}\text{Mn}_{0.1}\text{O}_2$ cathode did not exceed $\sim 125^\circ\text{C}$, and that of the coated Li_xCoO_2 exceeded $\sim 170^\circ\text{C}$. However, the Li-ion cells containing either cathode with the AlPO_4 -nanoparticle coating did not exhibit thermal runaway, although short-circuits occurred at 12 V during a 3 C overcharging rate. It is evident that the AlPO_4 -coating layer on the powder drastically reduced the violent exothermic reaction between the electrolyte and cathode, controlling the overall safety of the Li-ion cells.
© 2004 The Electrochemical Society. [DOI: 10.1149/1.1790511] All rights reserved.

Manuscript submitted September 8, 2003; revised manuscript received March 16, 2004. Available electronically September 27, 2004.

Along with the improvement in the electrochemical properties of Ni-based cathode materials ($\text{LiNi}_{1-x}\text{M}_x\text{O}_2$ where M = metals), thermal instability with respect to Li_xCoO_2 is a great concern for use in Li-ion cells.¹⁻¹² Ni-based cathode materials have not met the safety guidelines that require no explosions, fire, or smoke during the nail penetration test at a 4.35 V overcharged state in Li-ion cells.¹³ In terms of thermal stability, the violent exothermic reaction of the cathode with the electrolyte accompanying substantial heat generation should be avoided. Otherwise, it causes thermal runaway, exhibiting fire, sparks, and explosions.

To minimize oxygen evolution (heat generation), addition of Mg, Ti, or Al in LiNiO_2 was reported to be effective in reducing the exothermic reaction, but greatly sacrificed the discharge capacity.^{14,15} For example, a $\text{LiNi}_{0.7}\text{Ti}_{0.15}\text{Mg}_{0.15}\text{O}_2$ cathode showed 190 mAh/g even at the charged voltage of 5 V, and its specific capacity at a 4.3 V cutoff is smaller than LiCoO_2 .¹⁴ To overcome the thermal instability of Ni-based cathode materials, some additives (for example, γ -butyrolactone) were used to reduce the direct reaction of the cathode with the electrolyte at the charged states. This solvent was reported to decompose into the organic products, thereby encapsulating the cathode, blocking any direct reaction with the electrolyte.¹³ As a consequence, Li-ion cells containing this solvent did not explode during the nail penetration (at 4.35 V) and overcharge tests to 12 V. However, such an additive has raised concerns about its compatibility with the anode and cathode, which therefore still needs to tailor its electrochemical properties.

Recently, a more fundamental approach was used to improve the thermal stability of the cathode materials.¹⁶ Cho *et al.* demonstrated that a nanoparticle- AlPO_4 coating on the LiCoO_2 cathodes blocked the thermal runaway of the Li-ion cell, and significantly reduced the electrolyte oxidation as well as Co dissolution into the electrolyte. In this paper, we report the 12 V overcharge behavior of the AlPO_4 -coated LiCoO_2 and $\text{LiNi}_{0.8}\text{Co}_{0.1}\text{Mn}_{0.1}\text{O}_2$ in terms of their exothermic behavior.

Experimental

Synthesis of AlPO_4 -coated LiCoO_2 and $\text{LiNi}_{0.8}\text{Co}_{0.1}\text{Mn}_{0.1}\text{O}_2$.— LiCoO_2 was prepared from stoichiometric amounts of Li_2CO_3 and Co_3O_4 (average particle size of 2-3 μm). After mixing these starting materials using an automatic mixer for 2 h, the mixture was preheated at 600°C for 6 h, and thoroughly remixed again, followed by

firing at 900°C for 24 h. To coat the AlPO_4 nanoparticles on the LiCoO_2 cathode, 3 g of $\text{Al}(\text{NO}_3)_3 \cdot 9\text{H}_2\text{O}$ and 1.04 g of $(\text{NH}_4)_2\text{HPO}_4$ were dissolved and stirred in 20 g of water until a white AlPO_4 nanoparticle suspension was observed. LiCoO_2 (100 g) with an average particle size of $\sim 10 \mu\text{m}$ was added to the coating solution and thoroughly mixed for 5 min. The slurry was then dried in an oven at 120°C for 6 h and heat-treated in a furnace at 700°C for 5 h. Transmission electron microscopy (TEM) confirmed that the Al and P elements were confined within $\sim 10 \text{ nm}$ from the surface.¹⁶

The $\text{Ni}_{0.8}\text{Co}_{0.1}\text{Mn}_{0.1}(\text{OH})_2$ starting material consisting of spherical particles ($\sim 13 \mu\text{m}$ diam) was prepared by co-precipitation from a solution containing stoichiometric amounts of nickel and cobalt nitrates, and manganese nitrate by the addition of NaOH and NH_4OH solutions in the reactor.² The $\text{LiNi}_{0.8}\text{Co}_{0.1}\text{Mn}_{0.1}\text{O}_2$ was prepared by mixing stoichiometric amounts of LiOH and $\text{Ni}_{0.8}\text{Co}_{0.1}\text{Mn}_{0.1}(\text{OH})_2$, followed by heat-treatment at 800°C for 20 h in a stream of dried air. An excess amount of Li (1.02 mole) was used to compensate for the loss of Li during firing. The resultant powders showed a Brunauer, Emmett, and Teller (BET) surface area of $1 \text{ m}^2/\text{g}$. The process for AlPO_4 coating on the cathode is identical to the LiCoO_2 described above.

Preparation of test cells.—The cathodes for the battery test cells were made from the cathode material, Super P carbon black, and polyvinylidene fluoride (PVdF) binder (Kureha Company) in a weight ratio of 96:2:2. The electrodes were prepared by coating a cathode-slurry onto an Al foil followed by drying at 130°C for 20 min. The slurry was prepared by thoroughly mixing a N-methyl-2-pyrrolidone (NMP) solution of PVdF, carbon black, and the powdery cathode material. The coin-type battery test cells (size 2016) prepared in helium-filled glove box contained a cathode, a Li metal anode, and a microporous polyethylene separator. The electrolyte was 1 M LiPF_6 with ethylene carbonate/diethylene carbonate/ethylmethyl carbonate (EC/DEC/EMC) (30:30:40 vol %, Cheil Ind. Korea). We used standardized coin-cell parts (2016R-type), and normally the amount of the electrolyte was $\sim 0.1 \text{ g}$ in each cell. Each test cathode contained $\sim 25 \text{ mg}$ of either LiCoO_2 or $\text{LiNi}_{0.8}\text{Co}_{0.1}\text{Mn}_{0.1}\text{O}_2$. The test cells were aged at room temperature for 24 h prior to the electrochemical test. Cells with a dimension $3.4 \times 40 \times 62 \text{ mm}$ were used for the 12 V overcharging experiments, and the anode material was synthetic graphite. The dimensional ratio of anode to cathode (matching ratio) was 1.08:1 for the Li-ion cells. The overcharge test used the guidelines reported elsewhere.¹⁷ The cell-surface temperature was monitored using a

* Electrochemical Society Active Member.

^z E-mail: jpcho@kumoh.ac.kr

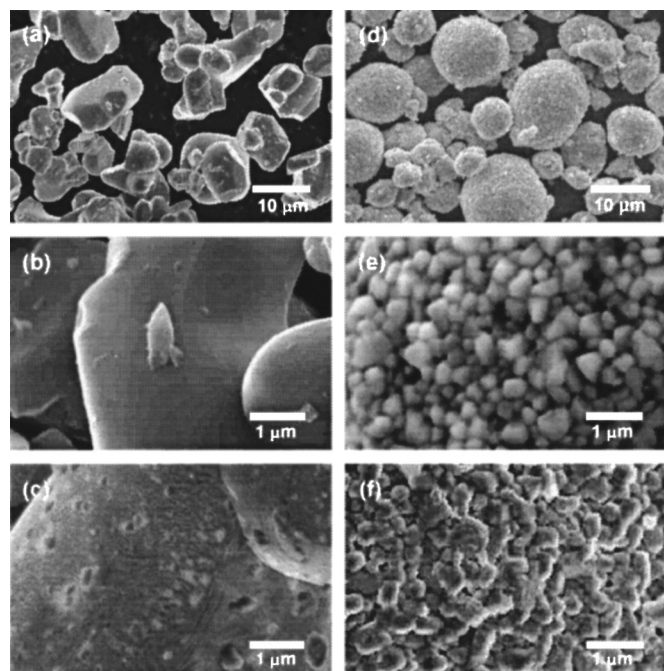


Figure 1. (a) and (b) SEM micrographs for bare LiCoO_2 , and (c) for AlPO_4 -coated LiCoO_2 . (d) and (e) Micrographs of bare $\text{LiNi}_{0.8}\text{Co}_{0.1}\text{Mn}_{0.1}\text{O}_2$. (f) Micrograph from AlPO_4 -coated $\text{LiNi}_{0.8}\text{Co}_{0.1}\text{Mn}_{0.1}\text{O}_2$.

K-type thermocouple placed on the center of the largest face in the cell can, and the thermocouple was tightly glued with insulating tape.

Electrochemical and DSC testing.—To compare the capacity of the AlPO_4 -coated LiCoO_2 with $\text{LiNi}_{0.8}\text{Co}_{0.1}\text{Mn}_{0.1}\text{O}_2$ cathode, coin-type half-cells were used with a charge cutoff voltage of 4.3 V at the charge and discharge rates with a constant current of 0.1 C (14 and 18 mA/g, respectively). The cycling tests of the Li-ion cells containing AlPO_4 -coated LiCoO_2 and $\text{LiNi}_{0.8}\text{Co}_{0.1}\text{Mn}_{0.1}\text{O}_2$ were carried out by charging and discharging the cells at a 1 C rate for 200 cycles at 21°C. The rate-capability tests of the Li-ion cells containing

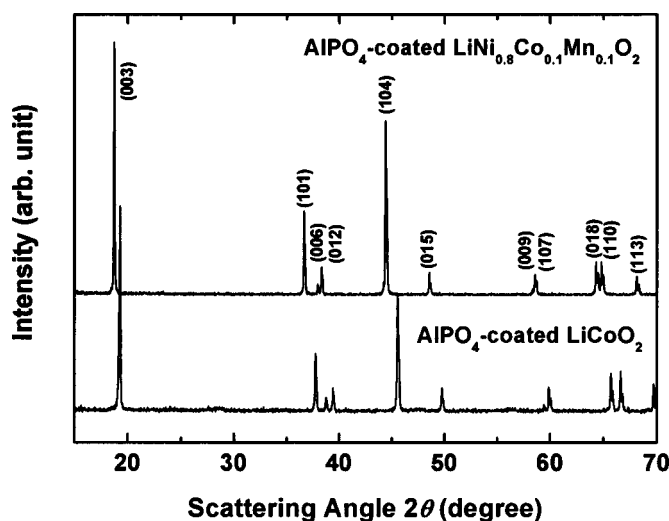


Figure 2. XRD patterns of the AlPO_4 -coated LiCoO_2 and $\text{LiNi}_{0.8}\text{Co}_{0.1}\text{Mn}_{0.1}\text{O}_2$ cathodes.

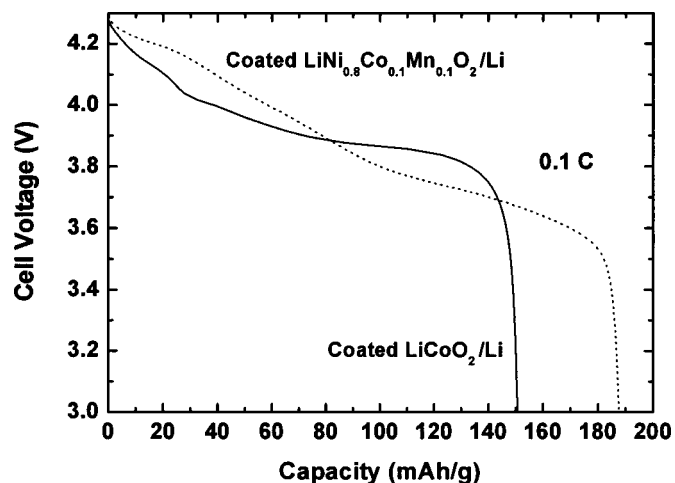


Figure 3. Plots of the first discharge curves from the AlPO_4 -coated LiCoO_2 and $\text{LiNi}_{0.8}\text{Co}_{0.1}\text{Mn}_{0.1}\text{O}_2$ cathodes in the coin-type half-cells between 4.3 and 3 V at 0.1 C rate (Li as an anode), while the 1 C rate corresponds to 140 and 180 mA/g, respectively.

AlPO_4 -coated LiCoO_2 and $\text{LiNi}_{0.8}\text{Co}_{0.1}\text{Mn}_{0.1}\text{O}_2$ were carried with a discharge rate of 0.5, 1, and 2 C (while the charge rate was fixed at 1 C).

The Li-ion cells for the differential scanning calorimetry (DSC) tests were charged to the pre-determined cell voltages, 4.2 and 4.6 V for bare cathodes, and 4.2, 4.4, 4.6, and 4.8 V for the coated cathodes at the constant-current mode of 1 C (710 and 820 mA for Li_xCoO_2 and $\text{Li}_x\text{Ni}_{0.8}\text{Co}_{0.1}\text{Mn}_{0.1}\text{O}_2$, respectively), which was followed by holding these voltages until the currents decreased to 30 mA. The charged cathodes were then disassembled from the cells in a dry room. The cathode electrode typically contained ~20 wt % electrolyte, ~25 wt % Al foil, a ~5 wt % combined binder and carbon black, and a ~50 wt % cathode material. Approximately 10 mg of the cathode was cut and hermetically sealed in an aluminum DSC sample pan. Only the cathode material was used to calculate the specific heat flow. The heating rate of the DSC tests was 3°C/min. Due to the high reactivity of the electrolyte with moisture, its content in the dry room was maintained below 50 ppm. Because the dry room was used for disassembling the cells for the DSC experiments, compressed DSC pans may contain oxygen. However, our DSC experiments up to 300°C showed negligible effects: pans assembled in the dry room were identical to those assembled in a glove box.

Results and Discussion

Scanning electron microscopy (SEM) images of the bare, AlPO_4 -coated LiCoO_2 and $\text{LiNi}_{0.8}\text{Co}_{0.1}\text{Mn}_{0.1}\text{O}_2$ cathode particles are shown in Fig. 1. The surface morphologies of both coated particles are distinctly different from those of the bare ones, and that of the coated $\text{LiNi}_{0.8}\text{Co}_{0.1}\text{Mn}_{0.1}\text{O}_2$ changed from a rough to smooth shape after the coating. This suggests that the AlPO_4 nanoparticles at least reacted at the surface of powders. A high-resolution TEM image of the coated LiCoO_2 showed the AlPO_4 nanoparticles embedded in a nanoscale-coating layer of ~10 nm. The nanoscale-coating layer consisted of random-oriented AlPO_4 nanoparticles with an average diameter of ~3 nm, and the Al and P components were distributed uniformly in the nanoscale-coating layer.¹⁶

Figure 2 shows the X-ray diffraction (XRD) patterns of AlPO_4 -coated LiCoO_2 and $\text{LiNi}_{0.8}\text{Co}_{0.1}\text{Mn}_{0.1}\text{O}_2$ powders. Both materials are indexed to the hexagonal-type space group $R\bar{3}m$. The lattice constants, a and c , for the AlPO_4 -coated LiCoO_2 material are $a = 2.815 \pm 0.004 \text{ \AA}$ and $c = 14.051 \pm 0.043 \text{ \AA}$ (with $2.816 \pm 0.004 \text{ \AA}$ and $14.034 \pm 0.043 \text{ \AA}$, respectively, for bare

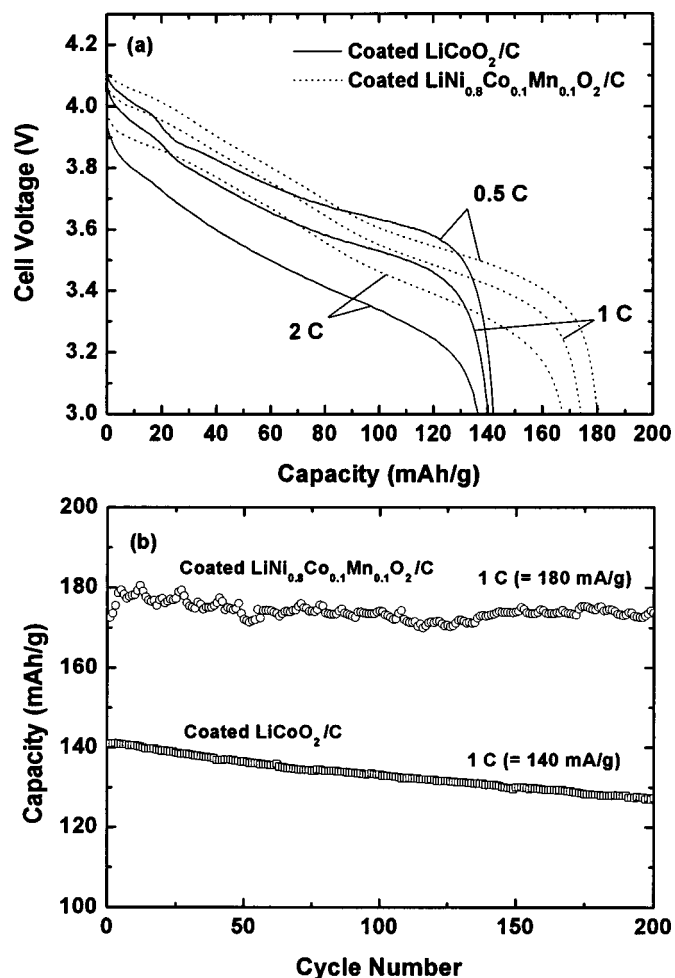


Figure 4. Plots of (a) the rate capabilities of the AlPO₄-coated LiCoO₂ and LiNi_{0.8}Co_{0.1}Mn_{0.1}O₂ cathodes in the Li-ion cells at 0.5, 1, and 2 C rates between 4.2 and 3 V, and (b) the discharge capacity as a function of the cycle number at 1 C rate.

samples), and those for the coated LiNi_{0.8}Co_{0.1}Mn_{0.1}O₂ material are $a = 2.874 \pm 0.001$ Å and $c = 14.217 \pm 0.008$ Å (with 2.877 ± 0.001 Å and 14.219 ± 0.003 Å, respectively, for bare samples). The XRD patterns of the coated LiCoO₂ or LiNi_{0.8}Co_{0.1}Mn_{0.1}O₂ powders are identical to those of the bare samples, even though the possible formation of nanophases or interdiffusion could not be ruled out.

To examine the electrochemical properties, coin-type half-cells with the coated LiCoO₂ and LiNi_{0.8}Co_{0.1}Mn_{0.1}O₂ were charged between 4.3 and 3 V at a rate of 0.1 C (14 mA/g and 18 mA/g, respectively). The first discharge curves in Fig. 3 show that the initial voltage profiles of the coated LiNi_{0.8}Co_{0.1}Mn_{0.1}O₂ cathodes above 4 V are higher than that of the coated LiCoO₂. The discharge capacity of the coated LiNi_{0.8}Co_{0.1}Mn_{0.1}O₂ is 188 mAh/g while that of the coated LiCoO₂ is 150 mAh/g. These values are identical to those of the bare cathodes. The larger discharge capacity of the LiNi_{0.8}Co_{0.1}Mn_{0.1}O₂ cathode than the coated LiCoO₂ is expected to increase the nominal capacity of the Li-ion cell.

The rate capabilities of the coated LiCoO₂ and LiNi_{0.8}Co_{0.1}Mn_{0.1}O₂ in the Li-ion full cells (between 4.2 and 3 V) are shown in Fig. 4a at a discharge rate of 0.5, 1, and 2 C (with the charge rate of 1 C). With relatively good capacity retention, the overall voltage profiles of the coated LiNi_{0.8}Co_{0.1}Mn_{0.1}O₂ appear enhanced as the C rate increased from 0.5 to 2 C, compared to the coated LiCoO₂. For the cycle-life performance, the coated

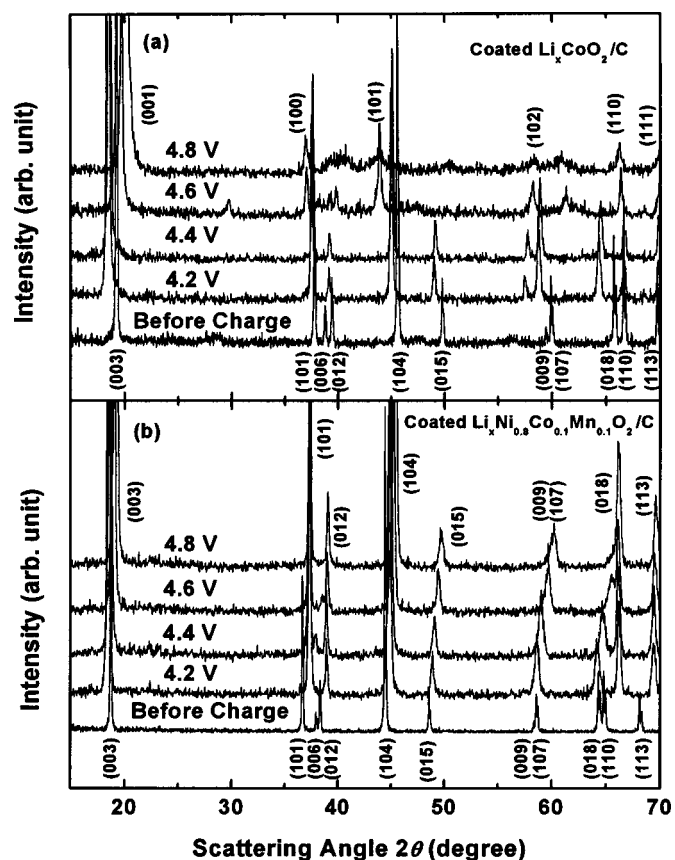


Figure 5. XRD patterns of (a) coated Li_xCoO₂, and (b) coated Li_xNi_{0.8}Co_{0.1}Mn_{0.1}O₂ cathode electrodes as a function of the charge voltage during the first charge.

LiNi_{0.8}Co_{0.1}Mn_{0.1}O₂ exhibits better capacity retention than the LiCoO₂ cathodes after 200 cycles, as shown in Fig. 4b.

Figure 5 compares the XRD patterns of the charged AlPO₄-coated Li_xCoO₂ and Li_xNi_{0.8}Co_{0.1}Mn_{0.1}O₂ cathode electrodes at 4.2, 4.4, 4.6, and 4.8 V in Li-ion cells (with carbon anode). In both cases, the (003) lines shift toward lower diffraction angles during the charge up to 4.2 V, and then shift back to the higher diffraction angles as the Li ions are further removed. At 4.8 V, the XRD pattern of the coated Li_xCoO₂ is indexed to the hexagonal unit cell in the space group of P3m1 (CdI₂ or O1 type). Because 4.8 V in the Li-ion cell corresponds to ~4.9 V vs. Li metal, the Li content in the Li_xCoO₂ is zero at 4.8 V. These results agree well with Ohzuku *et al.*¹⁸ and Amatucci *et al.*¹⁹ On the other hand, the XRD patterns of the coated Li_xNi_{0.8}Co_{0.1}Mn_{0.1}O₂ are indexed to the R $\bar{3}m$ (CdCl₂ or O3 type) space group even at a low Li content. Usually, the (101) and (104) peaks for a hexagonal lattice observed for LiNiO₂ were split into two peaks in the monoclinic lattice (C2/m).²⁰ However, these are not observed in the XRD patterns of the Li_xNi_{0.8}Co_{0.1}Mn_{0.1}O₂, which is similar to those of Li_xNi_{0.5}Co_{0.5}O₂ having a homogenous hexagonal phase transition.²⁰ Ohzuku *et al.* and Amatucci *et al.* reported that delithiated Li_xNiO₂ to $x \sim 0$ maintained the R $\bar{3}m$ structure without a monoclinic distortion at a low lithium content, which is unlike LiCoO₂.^{18,19} Similarly, the XRD patterns of Li_xNi_{0.8}Co_{0.1}Mn_{0.1}O₂ show that its structure at $x \sim 0$ (at 4.8 V) remains as R $\bar{3}m$.

A comparison of the AlPO₄-coating effect on the cathode materials was investigated using DSC. Figure 6 shows the DSC scans of the AlPO₄-coated and the bare Li_xCoO₂ cathodes in the Li-ion cells at different charge voltages. It shows continuous heat generation of

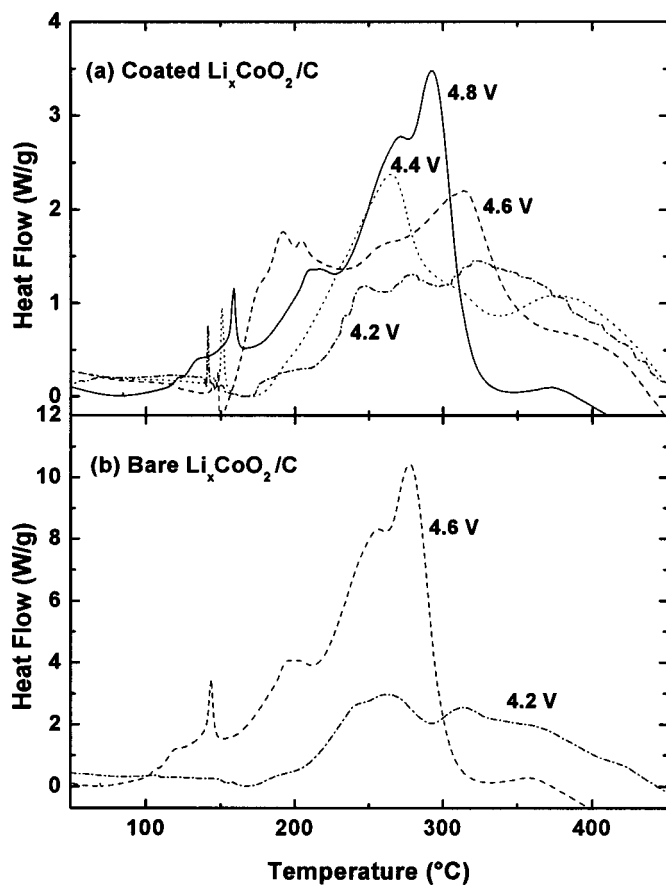


Figure 6. DSC scans of the coated and bare Li_xCoO_2 cathodes at different charge voltages. The cathodes were extracted from the Li-ion cells, and the scan rate was $3^\circ\text{C}/\text{min}$.

cathodes beginning at $\sim 150^\circ\text{C}$. As the charge voltage increases, the exothermic peak above 150°C , which is indicative of oxygen evolution from cathode decomposition, increases in both cathodes. The peak area of the coated LiCoO_2 cathode is approximately 2 to 3 times lower than that of the bare LiCoO_2 .

Figure 7 compares the DSC scans of the AlPO_4 -coated and the bare $\text{Li}_x\text{Ni}_{0.8}\text{Co}_{0.1}\text{Mn}_{0.1}\text{O}_2$ cathodes in the Li-ion cells at the different charge voltages. The coated $\text{Li}_x\text{Ni}_{0.8}\text{Co}_{0.1}\text{Mn}_{0.1}\text{O}_2$ shows two sets of exothermic peaks at ~ 75 and $\sim 200^\circ\text{C}$, which is similar to the bare ones. The peak at $\sim 75^\circ\text{C}$ may be related to the decomposition of organic compounds residing at the particle surface.^{21,22} Andersson *et al.*²¹ reported that the delithiated $\text{LiNi}_{0.8}\text{Co}_{0.2}\text{O}_2$ cathode surface contained a mixture of organic polycarbonates species, LiF or $\text{Li}_x\text{PF}_y\text{O}_z$ -type compounds, and electrolyte species due to high surface reactivity of the cathode powder.²³ A solid-electrolyte interphase (SEI) layer on delithiated electrodes containing various organic and inorganic electrolyte-decomposition products showed a mild heat generation below 100°C .²¹⁻²³

The DSC results suggest that the AlPO_4 -nanoparticle coating reduces heat generation during the electrochemical reactions. It should be noted that the peak size of the bare cathodes is significantly diminished after the AlPO_4 coating (Fig. 6 and 7). The BET surface area of all the samples were measured, and values from the LiCoO_2 and $\text{LiNi}_{0.8}\text{Co}_{0.1}\text{Mn}_{0.1}\text{O}_2$ powders were 0.6 and $1 \text{ m}^2/\text{g}$, respectively, whether the samples were coated or not. However, the DSC results showed significant heat reduction after the AlPO_4 coating, indicating that the crucial factor governing the exothermic reaction is the interfacial reaction with the electrolyte and cathode. With the surface reaction minimized by the coating, the oxygen generation inside the powders can be reduced. It is also believed that the

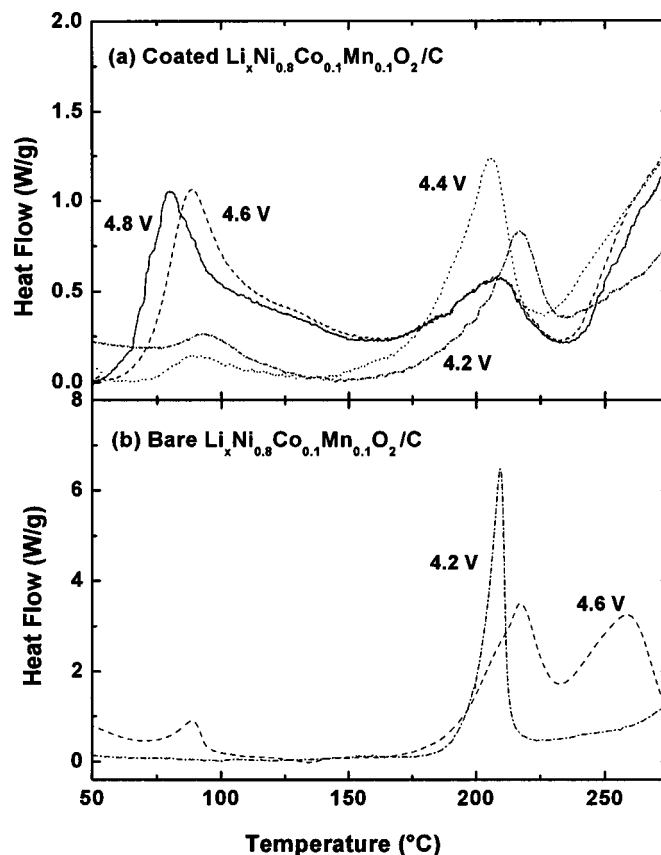


Figure 7. DSC scans of the coated and bare $\text{Li}_x\text{Ni}_{0.8}\text{Co}_{0.1}\text{Mn}_{0.1}\text{O}_2$ cathodes at different charge voltages. The cathodes were extracted from the Li-ion cells, and the scan rate was $3^\circ\text{C}/\text{min}$.

covalent-bond nature of $(\text{PO}_4)^{3-}$ with the Al cation contributes to a strong resistance to the reaction with the electrolyte. Oxides with $(\text{PO}_4)^{3-}$ bonding were reported to be thermally stable even at the fully delithiated state, and the MPO_4 ($\text{M} = \text{Fe}$ and Co) compounds exhibited a minimal weight loss from oxygen evolution when heated to 500°C .^{24,25}

The coated $\text{Li}_x\text{Ni}_{0.8}\text{Co}_{0.1}\text{Mn}_{0.1}\text{O}_2$ cathode exhibits more diffuse peaks than the coated Li_xCoO_2 with increasing cell voltage, suggest-

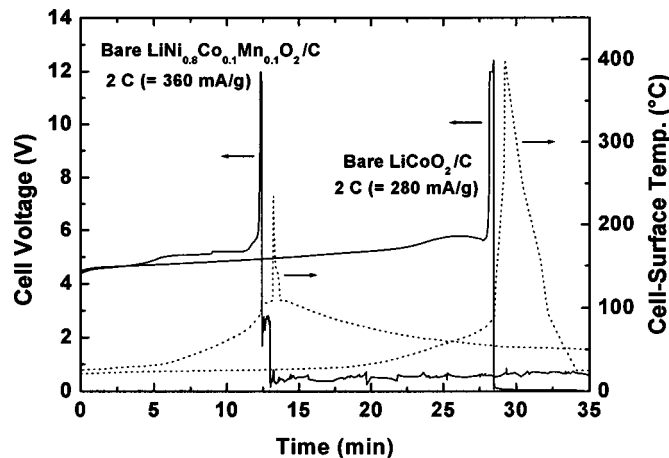


Figure 8. Plots of the cell voltage and cell-surface temperature in Li-ion cells containing the bare LiCoO_2 and $\text{LiNi}_{0.8}\text{Co}_{0.1}\text{Mn}_{0.1}\text{O}_2$ cathodes as a function of time at 2 C rate during the 12 V overcharge test.

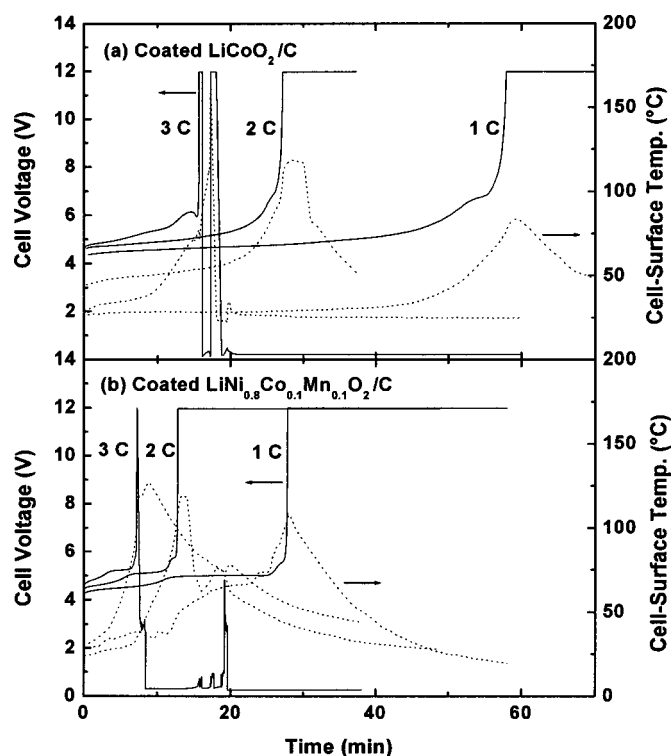


Figure 9. Plots of the cell voltage and cell-surface temperature in Li-ion cells containing AlPO_4 -coated LiCoO_2 and $\text{LiNi}_{0.8}\text{Co}_{0.1}\text{Mn}_{0.1}\text{O}_2$ cathodes at 1, 2, and 3 C rates during the 12 V overcharge test.

ing possibly slower reaction kinetics. This indicates that Li_xCoO_2 has a higher chance of undergoing thermal runaway compared to the $\text{Li}_x\text{Ni}_{0.8}\text{Co}_{0.1}\text{Mn}_{0.1}\text{O}_2$, with the competing heat-generation vs. heat-dissipation rates in Li-ion cells.²¹ To evaluate the effect of heat generation on the bare and AlPO_4 -coated LiCoO_2 and $\text{LiNi}_{0.8}\text{Co}_{0.1}\text{Mn}_{0.1}\text{O}_2$ in the Li-ion cells during the overcharge to 12 V, the cells were charged at three different current rates of 1, 2, and 3 C to 12 V (Fig. 8 and 9). At higher C rates, the cell-surface temperature increases rapidly due to the rapid increase in the joule heat, electrolyte oxidation, cathode decomposition, and other cell-component reactions. Among these, a violent exothermic reaction of the cathode with the electrolyte was reported to trigger thermal runaway of the cell.^{26,27} The Li-ion cell containing AlPO_4 -coated LiCoO_2 exhibits increasing cell-surface temperature with an increasing C rate: the cell-surface temperature reaches $\sim 170^\circ\text{C}$ at a 3 C overcharging rate. Because the difference between the internal and external temperature is $\sim 100^\circ\text{C}$ above 6 V,²⁶ the cell-internal temperature is estimated to be $\sim 270^\circ\text{C}$.

The AlPO_4 -coated $\text{LiNi}_{0.8}\text{Co}_{0.1}\text{Mn}_{0.1}\text{O}_2$ exhibits lower maximum cell-surface temperatures than the coated LiCoO_2 . This is due to faster heat dissipation than heat accumulation, which is consistent with the DSC results. A common feature of the coated LiCoO_2 and $\text{LiNi}_{0.8}\text{Co}_{0.1}\text{Mn}_{0.1}\text{O}_2$ is that a short-circuit occurred after shooting to 12 V at a 3 C rate charging. With the exothermic reactions of the cell components occurring within ~ 10 min, any direct contact between the cathode and the anode electrode can cause a short-circuit, which usually results in the thermal runaway of the cell containing a bare cathode.¹⁶ However, the surface temperature of the cell containing the coated $\text{LiNi}_{0.8}\text{Co}_{0.1}\text{Mn}_{0.1}\text{O}_2$ is limited to $\sim 125^\circ\text{C}$, lower than that containing the coated LiCoO_2 . Also, the AlPO_4 -coated $\text{LiNi}_{0.8}\text{Co}_{0.1}\text{Mn}_{0.1}\text{O}_2$ cathode reaches 12 V ~ 10 -30 min earlier than LiCoO_2 . This may be related to the different decomposition behaviors of the cathodes. When the first heat generation from the cathode particle induces a separator shutdown before the second heat generation begins at higher temperatures, the internal resistance of the

cell increases greatly. Eventually, this causes a decrease of current, resulting in a decrease in temperature. However, the coated LiCoO_2 cathode exhibits continuous heat generation beginning at $\sim 150^\circ\text{C}$ with a slimmer peak shape. Because this behavior causes faster heat accumulation than heat dissipation, the maximum cell-surface temperature at 12 V increases. This is well supported by the fact that the cell temperature of the bare LiCoO_2 cathode increases abruptly to $\sim 400^\circ\text{C}$ at 12 V upon short-circuiting, as shown in Fig. 8. However, a Li-ion cell containing bare $\text{LiNi}_{0.8}\text{Co}_{0.1}\text{Mn}_{0.1}\text{O}_2$ exhibits a maximum temperature of $\sim 225^\circ\text{C}$, accompanying only smoke from the bottom rupture of the can.

Conclusions

The DSC and 12 V overcharge tests demonstrated the enhanced thermal stability of the AlPO_4 -coated $\text{LiNi}_{0.8}\text{Co}_{0.1}\text{Mn}_{0.1}\text{O}_2$ cathodes compared to the AlPO_4 -coated LiCoO_2 . Although the reduced heat generation by the nanoparticle coating resulted in an improved thermal stability at high charge voltages, the distinctly separate heat generation with a wide temperature gap in the coated $\text{LiNi}_{0.8}\text{Co}_{0.1}\text{Mn}_{0.1}\text{O}_2$ plays a key role in decreasing the cell-surface temperature, unlike LiCoO_2 .

Acknowledgment

This work was supported by grant no. R05-2004-000-10029-0 from the Ministry of Science and Technology and KOSEF through the Research Center for Energy Conversion and Storage at Seoul National University.

Kumoh National Institute of Technology assisted in meeting the publication costs of this article.

References

1. K.-K. Lee, W.-S. Yoon, and K.-B. Kim, *J. Electrochem. Soc.*, **148**, A1164 (2001).
2. J. Cho, G. Kim, Y. Park, and S. Kim, U.S. Pat. 6,241,959 (2001).
3. Y. Nishida, K. Nakane, and T. Satoh, *J. Power Sources*, **68**, 561 (1997).
4. H. Watanabe, T. Sunagawa, H. Fujimoto, N. Nishida, and T. Nohma, *Sanyo Tech. Rev.*, **30**, 84 (1998).
5. Y. Sato, T. Koyano, M. Mukai, and K. Kobayakawa, Paper presented at The Electrochemical Society Meeting, Paris, France, Aug 31-Sept 5, 1997.
6. M. Yoshio, H. Noguchi, J.-I. Itoh, M. Okada, and T. Mouri, *J. Power Sources*, **90**, 176 (2000).
7. C. Nayze, F. Ansart, C. Laberty, J. Sarrias, and A. Rousset, *J. Power Sources*, **99**, 54 (2001).
8. J. Cho, T.-J. Kim, Y. J. Kim, and B. Park, *Electrochem. Solid-State Lett.*, **4**, A159 (2001).
9. J. Cho, H. Jung, Y. Park, G. Kim, and H. Lim, *J. Electrochem. Soc.*, **147**, 10 (2000).
10. J. Cho, G. Kim, and H. Lim, *J. Electrochem. Soc.*, **146**, 3571 (1999).
11. W. Li and J. C. Currie, *J. Electrochem. Soc.*, **144**, 2773 (1997).
12. H. Arai, M. Tsuda, K. Saito, M. Hayashi, and Y. Sakurai, *J. Electrochem. Soc.*, **149**, A401 (2002).
13. N. Takami, H. Inagaki, R. Ueno, and M. Kanda, Paper presented at the 11th International Meeting on Lithium Batteries, Monterey, CA, June 23-28, 2002.
14. Y. Gao, M. V. Yakovleva, and W. B. Ebner, *Electrochem. Solid-State Lett.*, **1**, 117 (1998).
15. I. Yoshiyuki, K. Kochichi, Y. Shuji, and K. Motoya, Paper present at The Electrochemical Society Meeting, Salt Lake City, UT, Oct 20-24, 2002.
16. J. Cho, Y. W. Kim, J.-G. Lee, B. Kim, and B. Park, *Angew. Chem., Int. Ed. Engl.*, **42**, 1618 (2003).
17. *Guideline for the Safety Evaluation of Secondary Lithium Cells*, Japan Battery Association (1997).
18. T. Ohzuku, A. Ueda, and M. Nagayama, *J. Electrochem. Soc.*, **140**, 1862 (1993).
19. G. G. Amatucci, J. M. Tarascon, and L. C. Klein, *J. Electrochem. Soc.*, **143**, 1114 (1996).
20. A. Ueda and T. Ohzuku, *J. Electrochem. Soc.*, **141**, 2010 (1994).
21. A. M. Andersson, D. P. Abraham, R. Haasch, S. MacLaren, J. Liu, and K. Amine, *J. Electrochem. Soc.*, **149**, A1358 (2002).
22. J.-I. Yamaki, H. Takatsuji, T. Kawamura, and M. Egashira, *Solid State Ionics*, **148**, 241 (2002).
23. S. C. Levy and P. Bro, *Battery Hazards and Accident Prevention*, Plenum Press, New York (1994).
24. A. K. Padhi, K. S. Nanjundaswamy, and J. B. Goodenough, *J. Electrochem. Soc.*, **144**, 1188 (1997).
25. S. Okada, S. Sawa, M. Egashira, J.-I. Yamaki, M. Tabuchi, H. Kageyama, T. Konishi, and A. Yoshino, *J. Power Sources*, **97**, 430 (2001).
26. R. A. Leising, M. J. Palazzo, E. S. Takeuchi, and K. J. Takeuchi, *J. Electrochem. Soc.*, **148**, A838 (2001).
27. H. Maleki, G. Deng, I. Kerzhner-Haller, A. Anani, and J. N. Howard, *J. Electrochem. Soc.*, **147**, 4470 (2000).